PHYSICAL REVIEW C VOLUME 43, NUMBER 3 MARCH 1991

Rainbow-shift mechanism behind discrete optical-potential ambiguities

M. E. Brandan
Instituto de Física, Universidad Nacional Autónoma de México, Distrito Federal, México 04510

K. W. McVoy
Department of Physics, University of Wisconsin, Madison, Wisconsin 53706
(Received 20 February 1990)

Some years ago, Drisko *et al.* suggested that the discrete ambiguity often encountered for elastic scattering optical potentials could be understood as being due to the interior or small-l S-matrix elements for two "equivalent" potentials differing in phase by 2π, l-by-l. We point out that the *absence* of this phase change for peripheral partial waves is equally essential, and suggest that a deeper understanding of the ambiguity may be achieved by viewing it as a consequence of a farside interference between interior and peripheral partial waves. It is this interference which produces the broad "Airy maxima" of a nuclear rainbow, and we show that a Drisko-type phase-shift increment $\delta_l \rightarrow (\delta_l + \pi)$ for low-l phases relative to the high-l ones is exactly what is needed to shift a farside rainbow pattern by one Airy maximum, thus providing an equivalent "rainbow-shift" interpretation of the discrete ambiguity. The physical importance of both interpretations lies in the fact that the existence of discrete ambiguities (as well as of nuclear rainbows) is explicit evidence for low-l transparency in nucleus-nucleus collisions. The essential role played by low partial waves explains why peripheral reactions have generally not proven helpful in resolving this ambiguity.

I. INTRODUCTION

A. Forward-angle potential ambiguities in elastic and inelastic data

Recent studies of elastic heavy-ion scattering have identified several systems, such as $^{12}C+^{16}O$, whose interactions are sufficiently transparent that their elastic angular distributions alone can eliminate continuous optical-potential ambiguities. However, if the angular range of the data is sufficiently restricted (e.g., to the region of Fraunhofer oscillations), the elastic data for these systems do admit discrete ambiguities, and in the few cases for which corresponding inelastic angular distributions are available, these discrete ambiguities are found to persist in them, as well.

These families of equivalent or ambiguous potentials have all been found via searches on one-channel optical potentials, or on optical potentials supplemented by distorted-wave Born approximation (DWBA) inelastic calculations. Their existence strongly suggests that equivalent discrete ambiguities would also be found by coupled-channel searches, but as far as we are aware, wide-ranging searches of this type have not yet been systematically attempted. The closely related question of whether discrete potential ambiguities in elastic data alone might be resolved by inelastic or transfer data is currently an open one, to which we return in Sec. VIII below. Independently of whether these ambiguities occur in elastic or inelastic data, however, their appearance in analyses of forward-angle data is a direct consequence of the "thin-skinned" radial shape of nuclear potentials.

To see this, recall that direct reactions are dominated, at current heavy-ion energies, by trajectory effects, and that trajectories are determined by classical-mechanics forces, i.e., by the potential derivative dV/dr. For typical nuclear potentials, of "squarish" radial shape, this force is largest in the surface region, $r \approx R$, and consequently it is the peripheral or grazing trajectories which are scattered to the largest angles. Hence forward-angle data are insensitive to the $r \approx R$ portion of the potential, and can be fit equally well by two or more such potentials, provided their derivatives differ only in the surface regions. It is exactly this insensitivity of forward-angle data to the surface region which is responsible for the occurrence of discrete potential ambiguities in V_0, the potential depth, since changing V_0 for a squarish potential shape changes dV/dr primarily in the surface region. Exactly which values of V_0 are admitted by specific forward-angle data is determined by an interference or rainbow phenomenon explained in Sec. IV below.

B. The l-space interpretation and the $(\delta + n\pi)$ farside ambiguity

The above trajectory interpretation of discrete ambiguities is clearly a semiclassical one, applicable only when kR, the number of active partial waves, is large. The low-energy data available when the first discrete ambiguities were noticed, in the early 1960's, were not amenable to this type of analysis, and in consequence Drisko, Satchler, and Bassel[1] were at that time lead to an alternative, l-space interpretation of these ambiguities.

These authors made the important observation that the occurrence of discrete ambiguities for a given target-projectile system is direct evidence for an important degree of "transparency" of this system, and they suggested the criterion that potentials V_1 and V_2 are "equivalent"

(i.e., provide equal-quality fits to the data) if

$$\delta(l,V_2)=\delta(l,V_1)+n\pi \tag{1.1}$$

is satisfied by the phase shifts of some *low-l* range of partial waves which contribute significantly to the scattering. We shall refer to this as the $(\delta+n\pi)$ criterion. It is primarily the real-potential depth V_0 which distinguishes these two potentials, and Eq. (1.1) implies that, as V_0 varies from V_{01} to V_{02}, $S(l,V_0)=e^{2i\delta(l,V_0)}$ makes n loops around the origin in the complex S-plane (in the increasing-phase direction if V_2 is deeper than V_1). It is precisely for the small-l waves that this is most likely to occur, since $|S(l,V_0)|$ is smallest for them: they are the S-matrix elements closest to the origin, and so can increase their phases by 2π with the smallest possible loops.

For the peripheral partial waves ($l \geq kR$), however, $S(l,V_0)$ is near 1, and is likely to remain there as V_0 varies. The only exception to this is the case in which deepening the potential moves a peripheral l-wave resonance downward in energy past the $E_{\text{c.m.}}$ of the beam, for this would indeed cause $\delta(l,V_0)$ to increase by π, for a real potential. However, peripheral-l resonances in a real potential are very narrow because they lie behind a high centrifugal barrier, and are inevitably "absorbed away" by the amount of imaginary potential encountered in realistic nuclear optical potentials. Consequently the above authors observed, astutely, that the peripheral phase shifts do not increase by π as V_0 varies between two equivalent values. This raises the interesting possibility that the change which occurs in an angular distribution, as V_0 is varied, is caused primarily by a change in an *interference* between low and high partial waves.

Our present purpose is to offer evidence that this indeed appears to be the case. We find that this interference occurs exclusively in the farside component of the scattering amplitude, where it produces the Airy maxima (A_1, A_2, etc.) of a nuclear rainbow. We further show that the Drisko *l-space* shift $\delta_l \rightarrow (\delta_l+\pi)$ produces, via this interference, a farside *angular* shift $A_m \rightarrow A_{m+1}$, which in turn causes the original angular distribution to reappear when V_{01} reaches V_{02}. It is precisely this "rainbow shift" (of one Airy maximum to the next) which explains Goldberg's important observation[2] that the ambiguity can be resolved if the dark-side falloff of the rainbow can be observed, forward of 180°. In whatever way one wishes to view this phenomenon, its most important physical implication is the one pointed out by Drisko *et al.*: the occurrence of discrete ambiguities is direct evidence of low-l transparency.

II. ^{6}Li+^{58}Ni AT 210 MeV: A NONRESONANT EXAMPLE

We draw our first example from the angular distributions recently published by Nadasen *et al.*[3] for the elastic scattering of 210-MeV ^{6}Li by a variety of targets, which provide a welcome addition to the growing systematics of light heavy-ion optical potentials.[4] Figure 1 displays the data for ^{6}Li+^{58}Ni, which we choose to examine in detail, and Fig. 2 shows the "deflection function" of the shallowest complex optical potential which fits the data, defined as

$$\Theta(l) \equiv 2\,\mathrm{Re}\left[\frac{d\delta}{dl}\right]. \tag{2.1}$$

If the real part of the optical potential has no single-particle or "shape" resonances near the bombarding energy under consideration, it is often found that this function is almost identical with the deflection function for the real part of the potential alone. Since this holds true in the present case, we feel confident in interpreting Fig. 2 as an accurate indication of which l values scatter into a given angle. In particular, the data we are concerned with are those forward of 35°, which come, according to Fig. 2, from a combination of the two disjoint angular momentum ranges $l<26$ and $l>40$. Figure 3(a) shows the phase shifts Re[$\delta(l)$] for three (complex) equivalent potentials ($V_0=174$, 266, and 360 MeV), which fit the $|\theta|<35°$ data equally well. Their cross sections are shown in Fig. 4(a), a nearside/farside decomposition of the $V_0=174$ MeV case is given in Fig. 4(b), and their full parameters are provided in Table I. We note from Fig. 3(a) that, in nice agreement with the $(\delta+n\pi)$ criterion, the phases for $l>40$ are nearly identical for all three po-

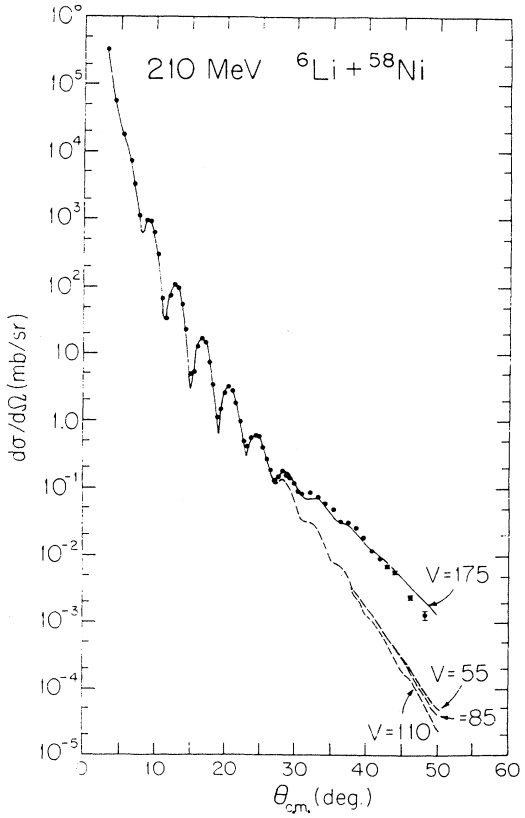

FIG. 1. Data of Nadasen *et al.* (Ref. 3), together with their discrete optical-model fits. The dashed curves were fitted only to the data forward of 27°.

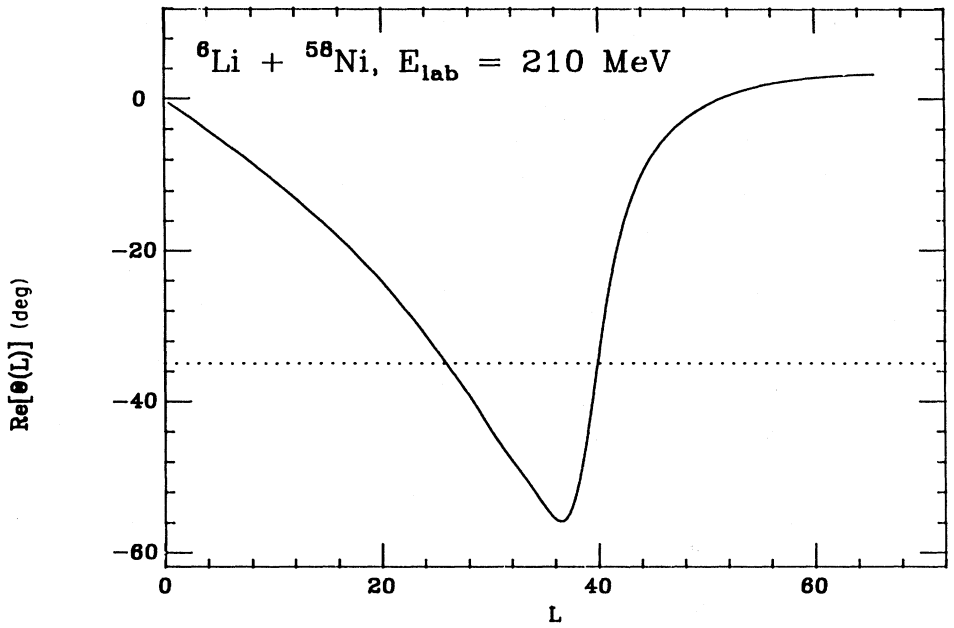

FIG. 2. The "deflection function" $2\,\mathrm{Re}(d\delta/dl)$, calculated for potential A_1 of Table I, from which it is seen that the angular region forward of 35° (dotted line) is determined by the partial waves $l<26$ and $l>40$. Extended-source Coulomb phase shifts are included in the calculation.

tentials, while those for $l<26$ increase by approximately π for $V_0=266$ MeV, and by 2π for $V_0=360$ MeV.

A. Weak versus strong absorption

In the following section we shall explain how the above observations relate to nuclear rainbows. Before doing so, however, we use the remainder of the present section to relate the farsides of the above scattering amplitudes to their underlying optical potentials (which are not, in fact, the potentials provided by Nadasen *et al.*), and to explain why we consider here only those data points lying forward of 35°, even though the measurements of the above authors extend to nearly 50°.

In the Nadasen energy range, where 40 or so partial waves contribute significantly and semiclassical concepts are applicable, current systematics[4,5] suggest that all heavy-ion optical potentials studied thus far fall into one of two categories, strongly-absorbing ($W_0 \gtrsim 40$ MeV; $|S(l=0)| \lesssim 10^{-4}$) or weakly absorbing ($W_0 \lesssim 40$ MeV; $|S(l)| \gtrsim 10^{-4}$). If only a limited, forward-angle part of the angular distribution is known, more than one potential is found to fit the data. These equivalent potentials differ most strikingly in the depth V_0 of their real part, and belong to either a continuous or a discrete family of ambiguities. The continuous or "Igo" ambiguity occurs for the strong-absorbing potentials. Since very little flux penetrates deeply into these potentials, it is not surprising that a continuous change in V_0 can be compensated by an appropriate change in the real geometry; the data only explore the surface region of the potential, and the members of a continuous family of strongly-absorbing potentials all have essentially the same real potential in the surface or tail region. It has also been noted[6] that the farside component of these angular distributions is a smoothly-decreasing function of scattering angle, devoid of any structure which might constrain the choice of potential parameters.

The weakly-absorbing potentials, in contrast, not only permit a deeper penetration of flux into their interiors, but also show significant structure in their farside angular distributions, the most common being the semiperiodic structure of a nuclear rainbow.[6] It is the data described by these "transparent" potentials which exhibit the discrete ambiguity, and a careful examination of the Nadasen data (among others) reveals that it is precisely the

TABLE I. WS parameters for ^{6}Li+^{58}Ni, $E_{lab}=210$ MeV.

Airy order	V_0	r_0	a	W_0	r_I	a_I
A_1	173.66	0.770	0.903	32.27	1.08	0.817
A_2	266.38	0.694	0.906	32.94	1.08	0.818
A_3	359.63	0.653	0.887	34.47	1.07	0.831

rainbow minima of their farsides which determine these discrete V_0 values, as we show in the following section. The Nadasen data actually cover a sufficiently extensive angular range that they *uniquely* determine an optical potential of the customary six-parameter Woods-Saxon form, so that no potential ambiguities are found for their full range of data.[3] However, these authors, realizing the importance of this uniqueness, took the unusual step of systematically discarding part of each angular distribution, by restricting it to a smaller and smaller (forward) angular range, in order to determine how small this angular range need be for two or more different potentials to provide acceptable fits.

For all six Nadasen targets (^{12}C, ^{28}Si, ^{40}Ca, ^{58}Ni, ^{40}Zr and ^{208}Pb) the unique potentials determined by the full angular range of the data were of the weak-absorption type in agreement with previous experience with alpha particles and other light projectiles. Consequently when the data were truncated sufficiently, the ambiguities which appeared were of the discrete type (excepting

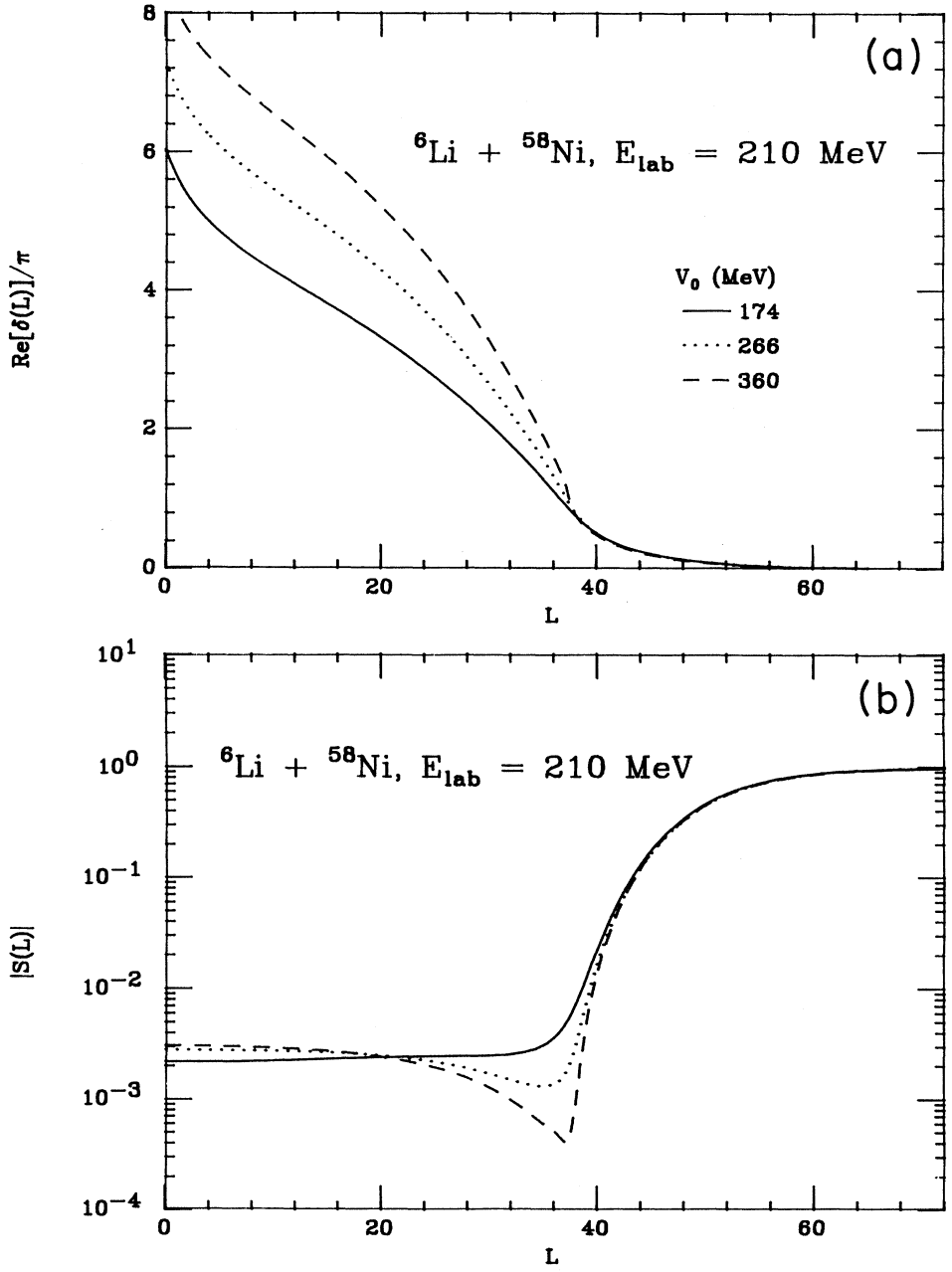

FIG. 3. (a) Real parts of the phase shifts for the equivalent optical potentials A_1, A_2, and A_3 of Table I, which differ by approximately π at $l \lesssim 20$. Extended-source Coulomb phases are included. (b) Magnitudes of $S(l)$ for the same potentials.

^{208}Pb, for which the angular region measured was very nearside-dominated), and the authors were able to locate two or three additional potentials of this type for each target.

However, the additional potentials found for the ^{58}Ni target were strongly absorbing ($W_0 > 57$ MeV), while those for all other targets were weakly absorbing. In addition, if the angular distributions were reproduced accurately for θ forward of some θ_0, then for $\theta > \theta_0$, the new potentials for C, Si, Ca, and Zr produced angular distributions that were higher than those of the original, unique, potential, at angles just beyond θ_0, but the new angular distributions for ^{58}Ni were lower, as Fig. 1 shows. They also correspond to values of V_0 which were smaller than that (174 MeV) of the original potential, while in all other cases the new V_0's were larger. We consequently felt it worthwhile to redo a search on the ^{58}Ni data (kindly provided by Dr. Nadasen). This search, done by insisting on a fit out to $\theta_0 = 35°$ rather than the 27° Nadasen employed, did in fact produce the low-χ^2 fits of Fig. 4(a); furthermore, it did so with weak-absorption, large-V_0 potentials very similar to those found by Nadasen for the other targets.

The reason behind the apparent discrepancy turned out to be interesting and important. It is indicated in Fig. 5, which compares three farside ($\Theta < 0$) angular distributions: the farside of the original potential, that of one of Nadasen's strong-absorption fits, and that of one of our weak-absorption fits. Consider first the original $V_0 = 174$ MeV potential fit, which we have purposely plotted out to angles somewhat beyond Nadasen's truncation at 27°. We do so to exhibit the fact that this farside (in common with those for all other targets) shows evidence of a nuclear rainbow, with a shallow Airy minimum at about 29° and a darkside exponential decay beyond about 40°. As we shall show below, the rainbow minimum at 29°, shallow as it is, is the "driving force" behind the weak-absorption fits for all Nadason targets, for all of them show such a minimum, including our $V_0 = 266$ MeV fit shown in Figs. 4 and 5. In locating this potential, in fact, it was essential that the full width of this farside minimum be included in the angular range searched, in spite of the fact that this minimum is "lost" under Fraunhofer (near/far) oscillations in the data themselves, as Fig. 1 shows. By restricting the angular range searched to $\theta < 27°$, Nadasen by chance truncated this farside minimum near its center. In this case, it becomes ambiguous whether the farside data beyond 27° will turn up, to define a minimum (as does the original 174 MeV potential), or will simply continue on with unchanged slope (on a log plot); this is, indeed, just the distinction between our $V_0 = 266$ MeV curve and Nadasen's $V_0 = 55$ MeV one. Furthermore, in order to achieve this smooth farside, with no hint of rainbow, his search was forced to employ absorption strong enough to damp out the Airy minimum completely.

In summary, this Airy minimum in the farside amplitude is found to play a crucial role in determining optical potential parameters, in agreement with analogous

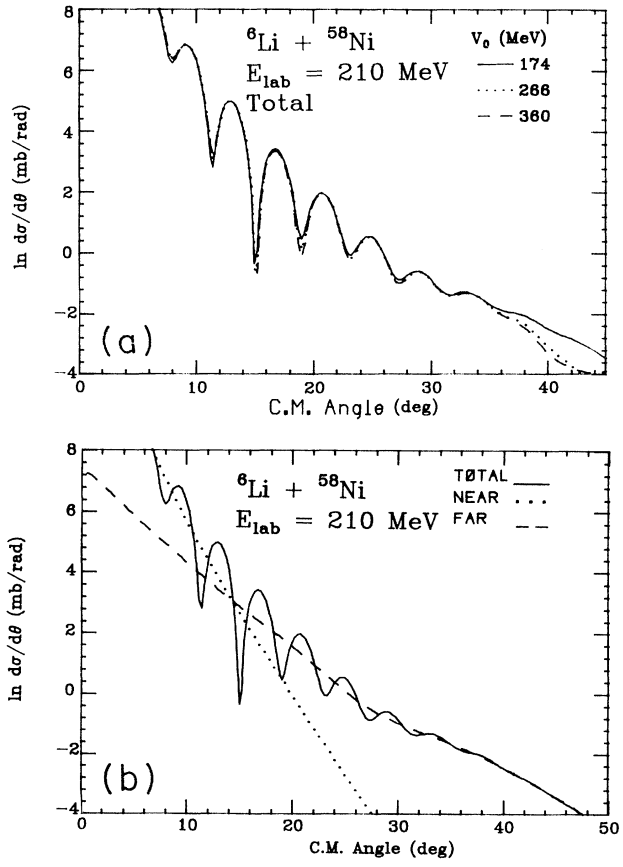

FIG. 4. (a) Optical potential angular distributions for the three equivalent potentials of Table I, which were fitted to the data of Fig. 1 forward of 35°. (b) A representative example of a near-side/far-side decomposition; this one is for the $V_0 = 174$ MeV potential of (a) (i.e., potential A_1 of Table I).

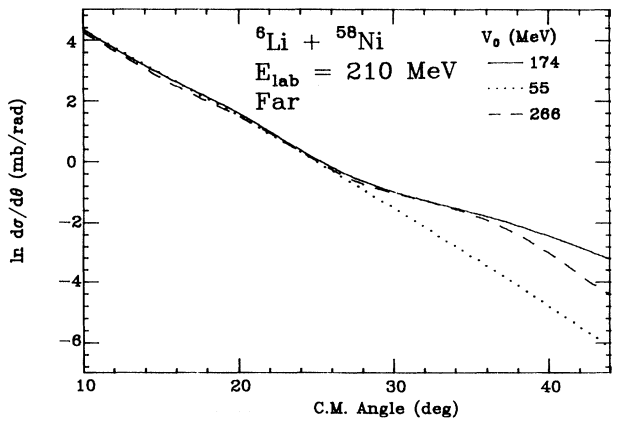

FIG. 5. Far-side cross sections of three optical potentials fitted to the data of Fig. 1. The solid and dashed curves (potentials A_1 and A_2 of Table I) were fitted to data forward of 35°, while the dotted curve was fitted to the data forward of 27°.

findings on other heavy-ion systems.[6] In fact, the importance of the farside minimum actually goes beyond that of the systems studied previously, both because the minimum (actually just a shoulder) itself is so shallow, and because in this case, unlike those examined in Ref. 6, it is hidden under the oscillations of the Fraunhofer crossover.

III. THE RAINBOW-SHIFT INTERPRETATION OF DISCRETE AMBIGUITIES

With the key role of the Airy minimum thus established, we restate the discrete-ambiguity question in terms of nuclear rainbows: Starting from the original value $V_0=174$ MeV, why does the fit deteriorate as V_0 is increased, and why do good fits "return" at the magic values of 266 and 360 MeV? The answer, fortunately, is nearly as obvious as the question, and becomes completely clear from Fig. 6, which shows the full farside angular distributions for these three potentials. Increasing the depth of an attractive potential increases its rainbow angle (negatively), thus shifting its farside pattern of Airy maxima and minima to larger angles. Moving the crucial first Airy minimum away from 29° will certainly worsen the fit to the data, but the farside Airy pattern is semiperiodic, and moving this pattern far enough will bring the *next* Airy minimum to 29°, where it restores the fit (though only for angles forward of about 35°, of course). Exactly this happens at $V_0=266$ MeV, and it happens again, with the following Airy minimum, at 360 MeV. It is thus simply the periodicity of the farside Airy pattern which makes the acceptable V_0 values discrete, and the Airy period is what fixes these magic V_0 values. We refer to this interpretation as the "rainbow-shift discrete potential ambiguity," and find that exactly the same phenomenon occurs in ^{6}Li scattering by the other targets of Nadasen *et al.* Perhaps the most remarkable of these cases is that of ^{28}Si, for which the relevant Airy minimum is reduced to an almost-invisible shoulder at 20°, shown in the farside plot of Fig. 7; it too lies under the Fraunhofer (near/far) interference oscillations of the data, which continue to 46°.

IV. RAINBOWS IN l-SPACE, AND THEIR RELATION TO $(\delta+n\pi)$

We thus appear to have two distinct interpretations of the discrete form of potential ambiguity, one in terms of phase shifts and the other in terms of a rainbow shift in angle. The central purpose of our discussion is to demonstrate that at sufficiently high (i.e., nonresonant) bombarding energies, these two interpretations are in fact identical. At low (resonant) energies, on the other hand, we find that the rainbow-shift interpretation continues to hold, whereas in some cases the Drisko or $(\delta+n\pi)$ interpretation fails, in a rather curious manner to be discussed in the following sections.

The nonresonant case will be examined in the present section, and to do so we begin with a brief review of the l-space description of rainbow scattering, using the ^{6}Li+^{58}Ni case as an example.

As mentioned earlier, we shall call

$$\Theta(l)\equiv 2\,\mathrm{Re}\left[\frac{d\delta}{dl}\right] \tag{4.1}$$

the "deflection function" for a complex potential, if we find it to be nearly the same function of (real) l whether the imaginary part of the potential is present or not; this is true in the present case. As in the example already noted in Fig. 2, it identifies the l values which scatter into a given θ, and the farside amplitude of each such (additive) contribution to $f(\theta)$ is given, in the semiclassical approximation, as

$$f_{\mathrm{far}}(\theta)=\frac{1}{k}\left[\frac{l}{\sin\theta\,\theta'(l)}\right]^{1/2} e^{i[2\delta(l)+l\theta]}, \tag{4.2}$$

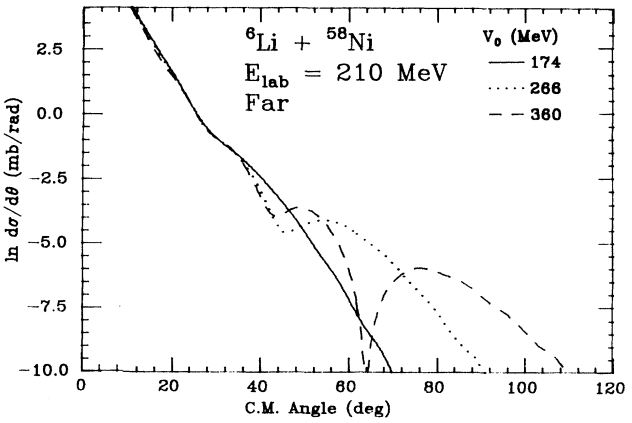

FIG. 6. The farsides for the three equivalent potentials of Fig. 4. The "Airy dip" at ≈29° is the first bright-side dip for potential A_1, the second bright-side dip for potential A_2, and the third bright-side dip for potential A_3, all of Table I.

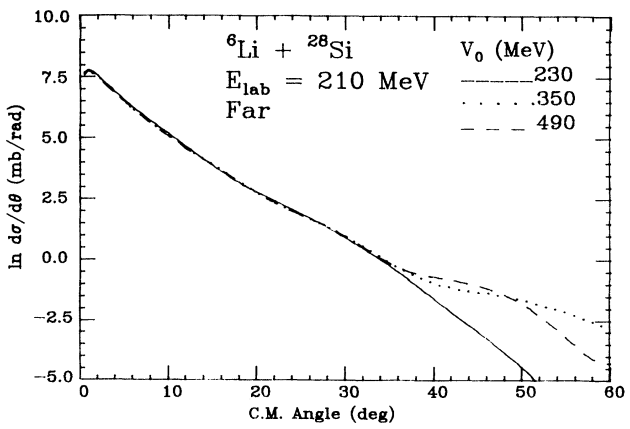

FIG. 7. Farside cross sections for three potentials fitted by the authors of Ref. 3 to a forward-angle portion ($\theta<30°$) of their data.

where θ is the measured scattering angle, a positive number, and l is a complex number satisfying $2\,d\delta/dl=-\theta$, as explained, e.g., in Ref. 7. Note that although $f(\theta)$ contains $\theta'(l)\equiv 2(d^2\delta/dl^2)$ as a factor, its magnitude $|f|$ is independent of $\mathrm{Re}[\delta(l)]$; in fact, if $\mathrm{Re}[\delta(l)]$ changes by π, without changing the shape of the deflection function $2\,\mathrm{Re}[\delta'(l)]$, this will leave $f_{\mathrm{far}}(\theta)$ entirely unchanged.

The deflection function of Fig. 2 shows that, in that example, it is the amplitudes with $l\approx 22$ and $l\approx 40$ which contribute to the scattering at $\theta=29°$, and since an Airy minimum (due to their interference) occurs there, they must be 180° out of phase. Assuming the phase of each

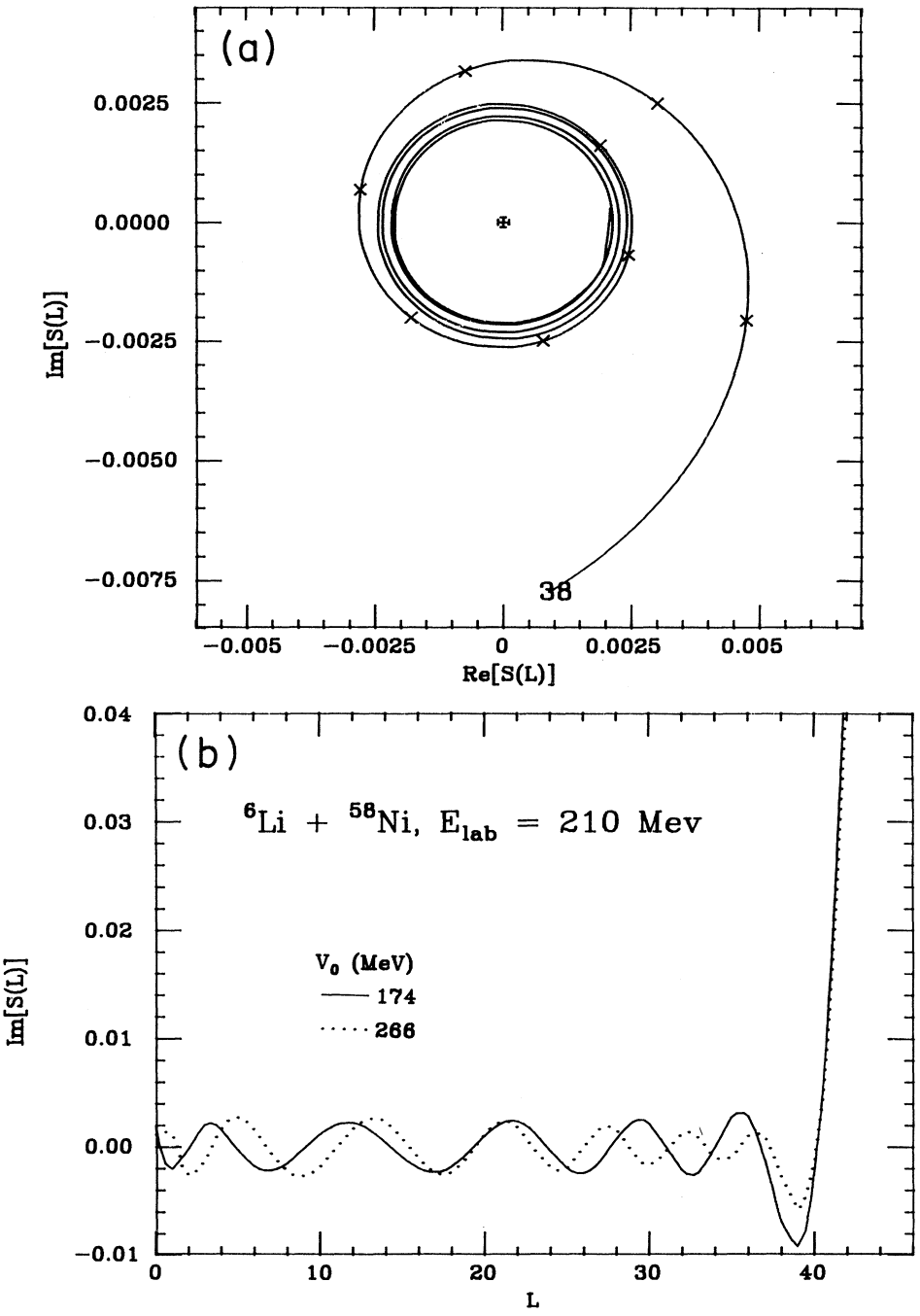

FIG. 8. (a) The Argand diagram for the $l\leq 38$ S-matrix elements of potential A_1 of Table I. The curve is calculated for continuous l; the $S(l)$ values for $l=30$ through 37 are marked by crosses. Note that $|S(l)|<0.01$ for all included points. (b) Projection of the circles of (a) onto the Im(S) axis, for potentials A_1 and A_2 of Table I. The curves are in phase at $l\approx 40$ and $l\approx 20$.

amplitude to come mainly from the exponential in (4.2), this requires

$$\mathrm{Re}[2\delta(l_<)-2\delta(l_>)+(l_<-l_>)\theta]=\pi \pmod{2\pi}, \quad (4.3)$$

where $l_< \approx 22$ and $l_> \approx 40$ in this case.

If V_0 is increased, the deflection function curve will deepen, moving its rainbow angle to a more negative value. Imagine for the moment that this could be accomplished [via an appropriate change in the shape of $V(r)$] in such a way that the wings of the deflection function, covering the angular range $\theta \lesssim 35°$, remained unchanged, with the change occurring only in the intermediate range $26 < l < 40$, corresponding to angles beyond 35°. Even though $d\delta/dl$ remains fixed in the forward-angle wings, $\delta(l)$ itself can increase for $l < 26$ by a constant (i.e., l-independent) amount as V_0 increases. That is, under these conditions the $(l_<-l_>)\theta$ term of Eq. (4.2) will remain constant, at a given θ forward of 35°, but $\delta(l)$ may steepen in the intermediate l range $26 < l < 40$, which is responsible for angles beyond 35°. In this case, $[\delta(22)-\delta(40)]$ will increase with V_0, and the Airy minimum will move from 29° to larger angles. [This can be seen directly from Eqs. (4.2) and (4.3) by noting that the dominant part of (4.3) is $[l_>\theta-2\delta(l_<)]$, so increasing $\delta(l_<)$ shifts any function of this argument in the direction of increasing θ.] If the low-l's change sufficiently that $[\delta(22)-\delta(40)]$ increases by exactly π, a new Airy minimum will have moved to 29°; this happens when V_0 reaches 266 MeV, and so restores the fit to the forward-angle data via a "rainbow shift." The condition for discrete rainbow-shift ambiguities is thus that V_0 increase just enough that

$$\mathrm{Re}[\delta(l_<)-\delta(l_>)] \quad (4.4)$$

increase by π. In the idealized case that $d\delta/dl$ is independent of V_0 for $l < l_<$, *all* phase shifts for $l < l_<$ will then increase by exactly π. This is precisely the $(\delta+n\pi)$ rule, applied to the small-l phases.

We have already seen in Fig. 3(a) how the $\mathrm{Re}[\delta(l)]$ curve does in fact change for the $V_0 = 174$, 266, and 360 MeV Woods-Saxon potentials. $\mathrm{Re}[\delta(40)]$, corresponding to the surface of the interaction region, remains nearly unchanged, but $\mathrm{Re}[\delta(l)]$ does increase with V_0 for lower l's, and the increase reaches π at $l \approx 19$, near the l-value corresponding to the 29° minimum. Within the constraints of the Woods-Saxon shape it is impossible to maintain this increase of exactly π for all smaller l's, though it could be accomplished by an appropriate change in the shape of $V(r)$.

Another way of viewing the same effect is to compare the full S-matrix elements for two equivalent potentials. For $l < 40$, the S-matrix elements are small, $|S(l)| \lesssim 0.04$, but as a function of l in this small-l range, they move around small circles in the decreasing-phase direction, in agreement with Fig. 3. Figure 8(a) displays these circles in the complex S plane (Argand diagram), and Fig. 8(b) shows their projection onto the $\mathrm{Im}(S)$ axis, for the $V_0 = 174$ and 266 MeV potentials. In the intermediate-l region, the "wavelength in l" is of course shorter for $V_0 = 266$ MeV, since its $|\mathrm{Re}(d\delta/dl)|$ is greater, but the two curves come back in phase at $l \approx 20$, corresponding to $\theta \approx 24°$, again close to the 29° farside Airy minimum. Exactly the same is found for $\mathrm{Re}[S(l)]$, and the same effect recurs for the $V_0 = 360$ MeV case.

In summary, these ^{6}Li+^{58}Ni data forward of 35° are determined by two (disjoint) l regions, $l < 26$ and $l > 40$, and it is their interference which produces the Airy minima of a nuclear rainbow in their farside amplitude. As V_0 is increased from 174 to 266 MeV, the phase shifts for $l < 26$ all increase by approximately π, in accord with the $(\delta+n\pi)$ criterion, whereas those for $l > 40$ remain essentially fixed. This changes the interference between the semiclassical amplitudes of these two l regions in just such a way as to shift one Airy minimum to the next (a shift of some 18° in this case), thus showing that the $\delta \to (\delta+n\pi)$ shift for low l's (only) is entirely equivalent to the rainbow-shift interpretation of the discrete potential ambiguity in this case. As we shall see below, the essential physical condition for this to be true is that the

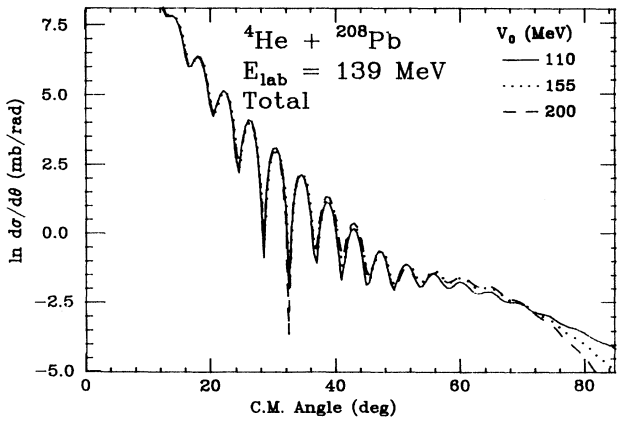

FIG. 9. Cross sections for the three equivalent optical potentials fitted by the authors of Ref. 8 to their data.

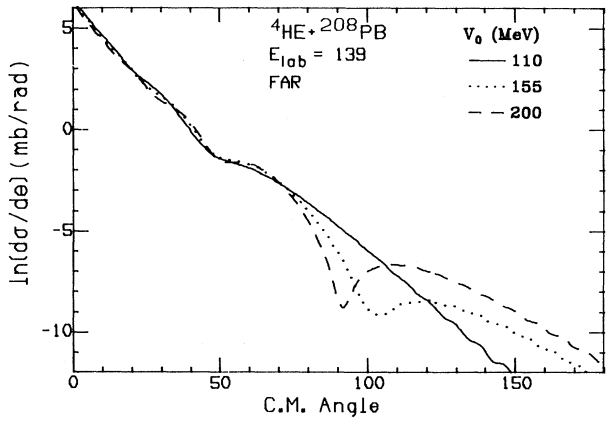

FIG. 10. Farside cross sections for the three equivalent optical potentials of Fig. 9. All three fit the Airy minimum at 50°. The rainbow angle of the dashed curve is well beyond 180°.

bombarding energy be sufficiently large that it is higher than the tops of all potential barriers in the effective potential $V_l(r)$: i.e., the scattering must be above the energy range of potential or shape resonances.

V. $\alpha+^{208}$Pb AT 139 MeV: THE RAINBOW SHIFT AND $(\delta+n\pi)$ IN THE PRESENCE OF POTENTIAL RESONANCES

A classical example of discrete ambiguities is the $\alpha+^{208}$Pb scattering measured at 139 MeV by Goldberg *et al.*[8] over the angular range $\theta<80°$. The three discrete fits that they found to their data are shown in Fig. 9, and the corresponding farside cross sections are shown in Fig. 10. By plotting these farsides well beyond the 80° limit of the data, it becomes clear that they are also rainbow-dominated, like those for ^{6}Li$+^{58}$Ni, and that in this case it is an Airy minimum at 50° which is the principal determinant of the equivalent-potential parameters.

The l-space story is somewhat more complex in this case, because the bombarding energy is low enough to encounter shape resonances of the real part of the optical potential. This is made evident by Fig. 11, which shows the l-dependence of the phase shifts resulting from the real parts only of the three equivalent optical potentials. They have been calculateed in steps of 0.002 in l, in order to locate the sharp steps of π seen at $l\approx43.2$ and 45.2, which mark Regge poles of shape resonances of the potential.

Figure 12 provides the deflection function $\Theta(l)=2[d\delta/dl]$ for the real part only of the weakest ($V_0=110$ MeV) potential. Although its central region, corresponding to large negative deflection angles, is dominated by two (overlapping) resonances and so is untrustworthy as a true deflection function, its wings, corresponding to angles forward of 70° or so, are smooth enough to identify the l values which scatter into these angles. In particular, it shows that the critical 50° farside Airy minimum arises from a destructive interference between $l\approx36$ and $l\approx43$.

Figure 11 shows that $\delta(36)$ increases by π as V_0 is increased from 110 to 155 MeV, but it also shows that this same increase in V_0 moves a resonance (it is the $n=0$ one) from $l\approx42$ to $l\approx43.2$, thus *also* causing $\delta(43)$ to increase by about π. This violates the condition of Eq. (4.4), that the difference $[\delta(l_<)-\delta(l_>)]$ should increase by π in order to move one Airy minimum to the next—and indeed an inspection of the cross sections (not shown here) for these two *real* potentials indicates that they are not equivalent at all.

However, these increases of π in $\delta(36)$ and $\delta(43)$, as V_0 increases, both correspond to excursions of their S-matrix elements around the full unit circle, as they must for real potentials. As might be anticipated, the sizes of these V_0 loops decrease drastically when realistic absorption ($W_0\approx21$ MeV) is included, since absorption makes $|S|<1$ and decouples resonances from this entrance channel. The resulting V_0 loops are illustrated by Fig. 13, where they are calculated by linearly interpolating ten intermediate values of each of the six Woods-Saxon potential parameters between their values for the 110 and 155 MeV potentials. For clarity, we only show the loops for $l=36$, 37, and 38. All those for $l<38$ do encircle the origin and so increase their phases by 2π, while all those

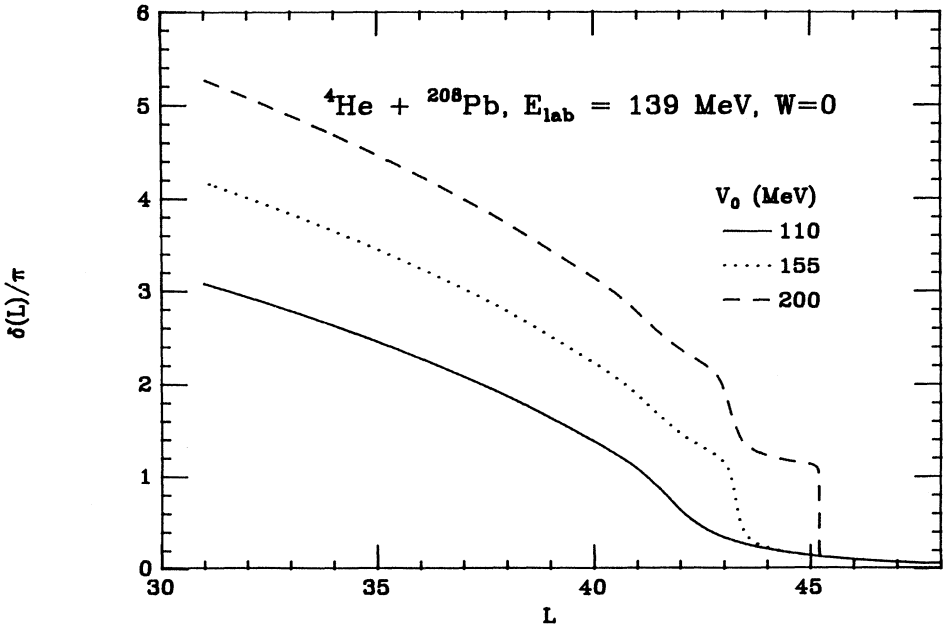

FIG. 11. Phase shifts, including extended-source Coulomb phases, calculated using the real parts only of the three equivalent optical potentials of Fig. 9. Note that they differ by π for $l\approx35$. The "steps" mark resonances degenerate at this energy.

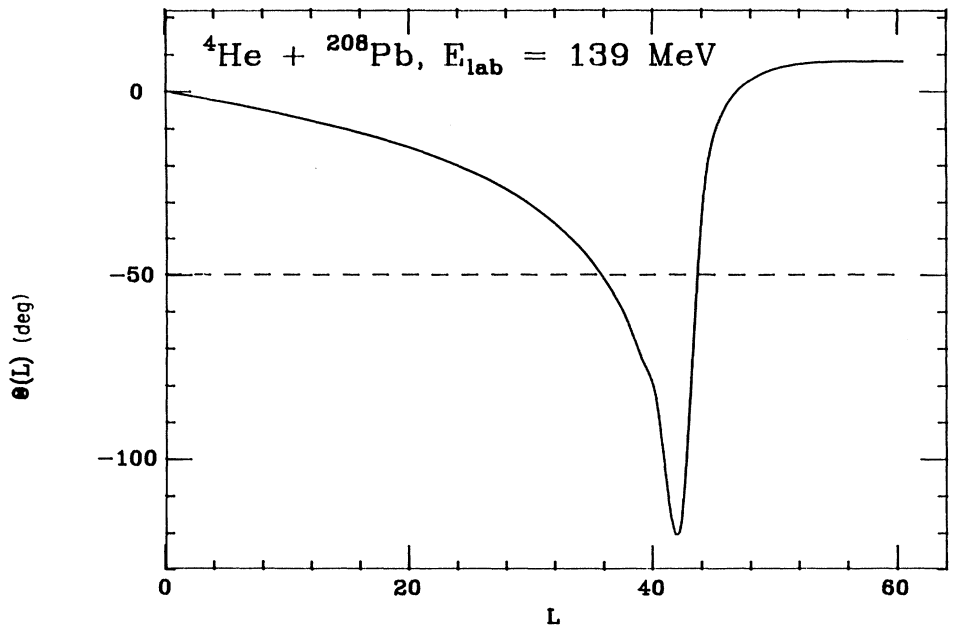

FIG. 12. The deflection function $\Theta=(2d\delta/dl)$ calculated from the solid curve of Fig. 11. The dashed line at $-50°$ marks the position of the Airy minimum which is critical in determining the equivalent potentials of Figs. 9 and 10.

for $l \geq 38$ do not. [That for $l=43$ is centered at (0.10,0.17) and so is off scale in Fig. 13.] It is via this "dance of the loops" that the presence of absorption, together with an increase in V_0, satisfies the condition that $[\delta(l_<)-\delta(l_>)]$ increase by π, and so shifts the rainbow pattern from one Airy minimum to the next.

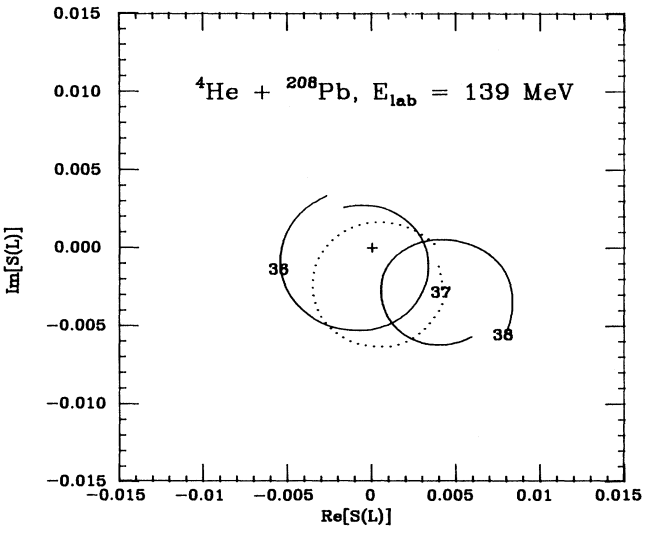

FIG. 13. Discrete-ambiguity loops for $l=36$, 37, and 38. The endpoints of each loop mark the value of $S(l,V_0)$ for the $V_0=110$ and 155 MeV equivalent potentials of Fig. 9; the points along the loops are calculated by linearly interpolating potential parameters between these limits. (If the equivalence were exact, the loops would close.) Since the $l=38$ curve does not encircle the origin, $S(38)$ does *not* increase its phase as V_0 increases from 110 to 155 MeV.

VI. $d+^{90}$Zr AT 11.8 MeV: $(\delta+n\pi)$ FAILS

The most unusual case of discrete ambiguities we have encountered so far is the original example cited by Drisko *et al.*, for which the $(\delta+n\pi)$ criterion seems, in fact, to fail completely.

The l dependence of the phase shifts for the real parts only of their two equivalent potentials is shown in Fig. 14, and is seen to be entirely dominated by resonances (Regge steps), as might be expected at an energy this low. Between $l=0$ and $l=9$ the $S(l)$ for the weaker potential is seen to make three decreasing-phase circuits around the unit circle, and that for the stronger potential makes four.

Because the resonances present are so narrow, they are very rapidly decoupled from this entrance channel by absorption, either reducing the $S(l)$ circles to very small loops or removing them altogether. Similarly, the $S_l(V_0)$ loops which each S_l follows as (V_0,W_0) is increased from (59.2, 7.7) to (86.13,9.5) (the values for the Drisko equivalent potentials) also shrink drastically. To our surprise, we find by directly calculating these loops for (V_0,W_0) values interpolated between these limits that, in fact, *none* of the V_0 loops encircle the origin, so none of the phase shifts increase by π in this case; Fig. 15 shows a few low-l examples.

What about the rainbow-shift interpretation in this case? At this low an energy, where $kr\approx 6$, $ka\approx 1$ and $\delta(l)$ is resonance-dominated in the absence of absorption,

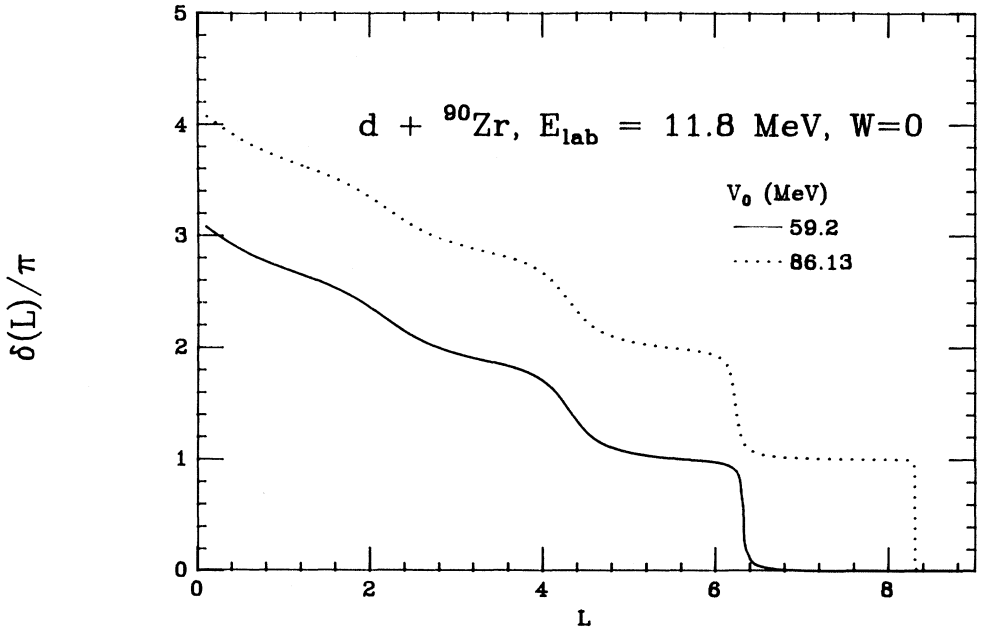

FIG. 14. Phase shifts, including extended-source Coulomb phases, calculated from the real parts only of the two equivalent potentials of Ref. 1, showing a difference between them of approximately π.

semiclassical approximations are unreliable, and we have no trustworthy deflection function for guidance. However, the nearside/farside decomposition of the angular distribution shown in Fig. 16 clearly shows a farside with Airy-like structure (though of course with the rainbow angle well beyond 180°).

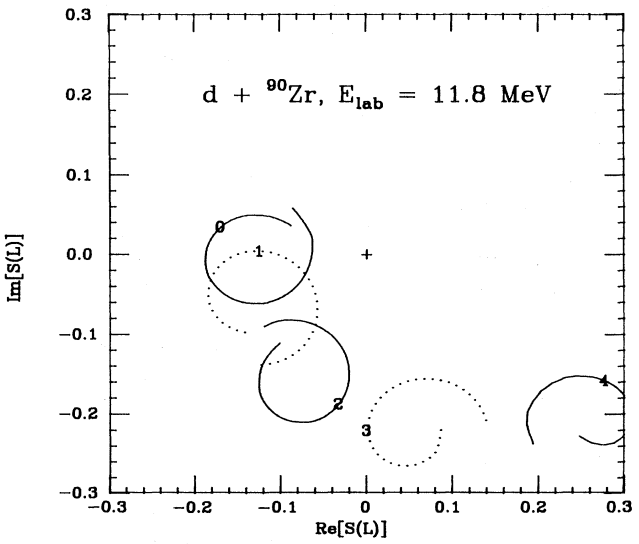

FIG. 15. Discrete-ambiguity loops, for $l=0$ through 4, for the two equivalent optical potentials of Ref. 1. The end-points mark $S(l,V_0)$ for the two equivalent potentials, and the curves show the path followed as the potential varies between these limits. Since none of the loops encircle the origin, none of the phase shifts satisfy $\delta_l \rightarrow (\delta_l + \pi)$ for the two equivalent potentials.

The farside cross section is at least a factor of 10 smaller than the nearside one at this Coulomb-dominated energy, but even so we can ask whether the farside minima are essential in determining the two equivalent potentials. Figure 17 appears to give a very positive answer, for it shows that the farside minima line up precisely for the two equivalent potentials, and are out of phase with those of a potential midway between them: Peculiarly enough, the original discrete-ambiguity example fails the $(\delta + n\pi)$ test, but does show a clear farside rainbow shift. This might at first sight seem to violate the argument given in Sec. IV, but in fact the semiclassical amplitude of Eq.

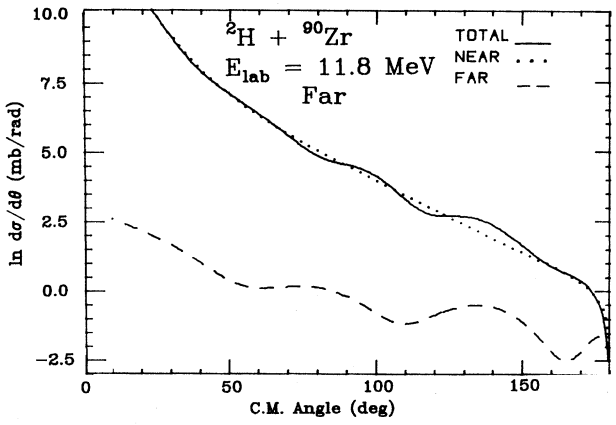

FIG. 16. Nearside/farside decomposition for the cross section of the 86.13 MeV potential of Ref. 1. Note the Airy-like oscillations of the farside, with a period approximately 1.7 times larger than that of the Fraunhofer oscillations.

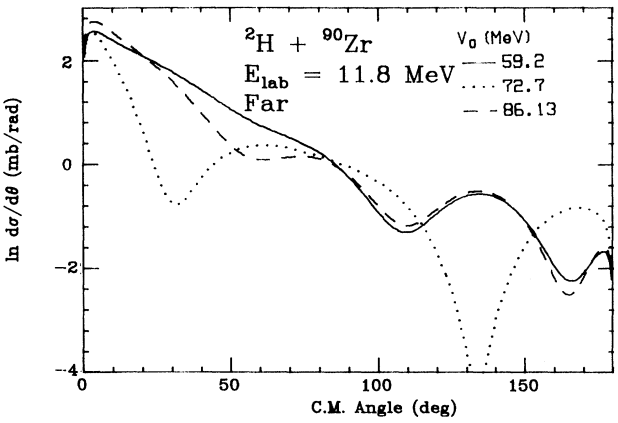

FIG. 17. A comparison of three farside cross sections for $d+^{90}Zr$. The solid and dashed curves are for the two equivalent potentials of Ref. 1, and are in phase. The dotted curve is for the arithmetic mean of these two potentials, and is seen to be out of phase with the first two: its potential strength is only great enough to move the Airy pattern halfway to that of the stronger potential.

(4.2) is invalid at an energy this low; we know of no simple argument to explain the appearance of an Airy-like farside pattern at this nonsemiclassical energy.

Figure 18 demonstrates explicitly that the sensitivity of the angular distribution to V_0 is entirely restricted to its farside, by comparing the nearsides for the three potentials of Fig. 17. All three curves are essentially identical, including that for $V_0=72.7$ MeV, whose farside is exactly out of phase with those of the two equivalent potentials. This same nearside invariance holds true for all the systems discussed in this article.

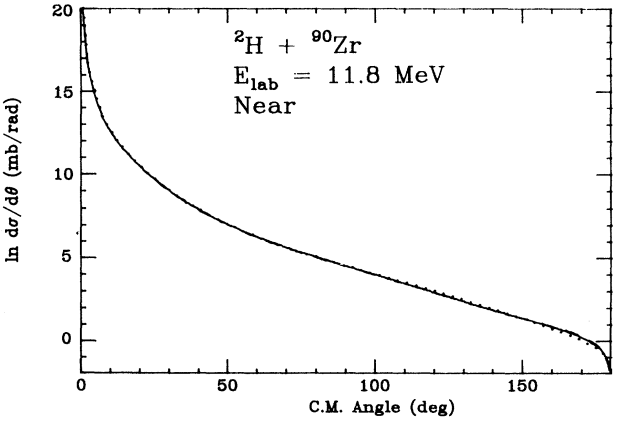

FIG. 18. A comparison of the three nearsides for the potentials of Fig. 17 (including the nonequivalent one). The near identity of the three curves shows that the effect of the potential changes is restricted almost entirely to the farside component.

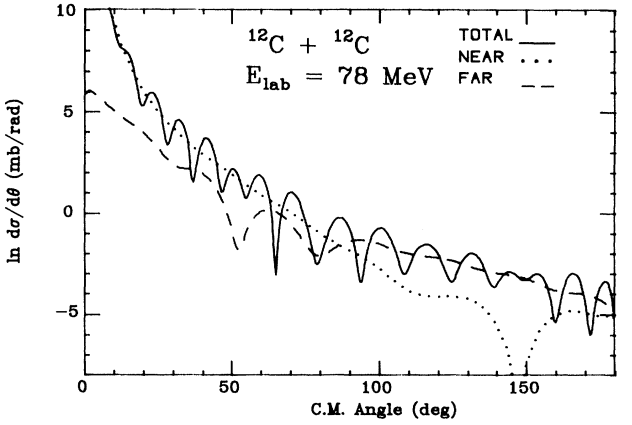

FIG. 19. Near-side/far-side decomposition of potential A_1 of Table II; in spite of the identity of target and projectile, the scattering amplitude has artificially not been symmetrized about 90°.

VII. IDENTICAL NUCLEI: $^{12}C+^{12}C$ AT 78.9 MeV

A recent study[9] of $^{12}C+^{12}C$ elastic scattering in the 100 MeV range shows that above 100 MeV the Fraunhofer oscillations weaken for $\theta_{c.m.} \gtrsim 40°$, while the oscillations arising from the identity of the nuclei do not begin until $\theta_{c.m.} \gtrsim 65°$, and the intervening angles show distinct indications of a farside Airy minimum, as noted in Ref. 4. Below 100 MeV, however, the Fraunhofer and symmetrization oscillations run continuously in each other, leaving no clear signs of the possible presence of Airy maxima or minima. Consequently the data in this energy range provide an interesting test case: does the rainbow shift play any role when its Airy pattern, if present, is buried beneath a *combination* of Fraunhofer and symmetrization oscillations?

Figure 19 provides the nearside/farside decomposition for the non-symmetrized cross section of the shallower of

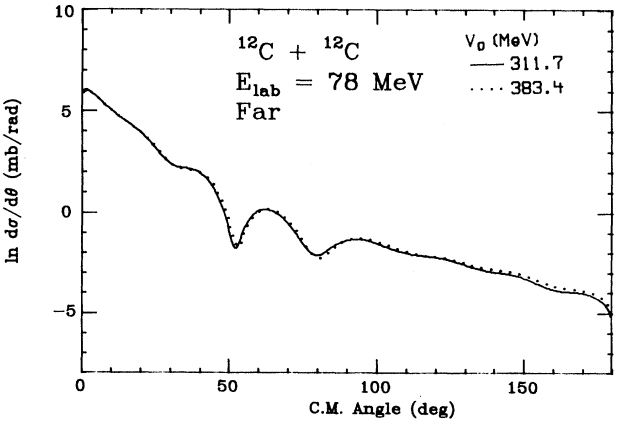

FIG. 20. A comparison of the two (nonsymmetrized) farside cross sections for the potentials of Table II.

TABLE II. WS parameters for $^{12}C+^{12}C$, $E_{lab}=78.9$ MeV.

Airy order	V_0	r_0	a	W_0	r_I	a_I
A_1	311.7	0.58	0.852	9.17	1.402	0.324
A_2	383.4	0.58	0.817	9.86	1.389	0.337

the two potentials found[9] to fit the data at $E_{lab}=78.9$ MeV (i.e., potential A_1 of Table II, which is the one found in Ref. 9 to best fit the potential systematics for the data studied there). Its farside component shows distinct minima at 80°, 52°, and possibly 30°, 110°, and 160°. We find analogous minima in the farside components at the other energies studied in Ref. 9, and from their motion with energy (not shown here), it is clear that they are indeed Airy or rainbow minima.

Figure 20 compares the farsides of the two equivalent potentials specified in Table II, showing that, in spite of the 20% difference in real depth, the two farsides are remarkably in phase. This is clear evidence that the discrete ambiguity, even in this identical-nucleus case, is due to an underlying rainbow shift. From the systematics of the farsides provided by the other potentials of Ref. 9 it would appear that the faint minimum at 160° is the first Airy minimum forward of the dark side for the A_1 potential of Table II, and the second minimum for the A_2 potential. The 52° minimum is then the fourth for the A_1 potential and the fifth for the A_2 potential. It is interesting to note that this 52° minimum does have an effect on the unsymmetrized angular distribution of Fig. 19, which is to make the two Fraunhofer minima at 48° and 55° shallower than the adjacent ones. This effect survives symmetrization, and is present in the data themselves.

In this context we recall that several years ago, Rowley, Doubre, and Marty[10] called attention to the occurrence of an unusual 90° minimum in the angular distribution for elastic $^{12}C+^{12}C$ scattering at 102 MeV. It is due to a deep farside Airy minimum occurring just at 90°, and was appropriately cited by these authors as strong evidence for important contributions coming from low partial waves, just as the occurrence of discrete ambiguities provides independent evidence of the same effect.

VIII. POTENTIAL AMBIGUITIES IN COUPLED-CHANNEL ANALYSES

To the best of our knowledge, all examples of discrete potential ambiguities known to date have been found by optical-potential searches on elastic data alone. The rainbow-shift explanation of these ambiguities shows them to be intimately tied to the trajectory concept, and since trajectories are also an essential feature of other direct reactions, two related and currently active questions suggest themselves.

(a) Can supplementary direct-reaction data, like that for inelastic scattering or transfer, resolve discrete elastic ambiguities?

(b) If such data are available, are coupled-channel parameter searches a feasible means of investigating this question?

In its simplest form, the first question asks whether Airy maxima also occur in inelastic and transfer farsides, and whether the relative weightings of their interfering trajectories are sufficiently different from those of elastic amplitudes that the reaction data might (in the same angular range) distinguish between elastically-equivalent potentials. In partial answer, we cite three recent studies, whose conclusion is that inelastic scattering is too surface-peaked to be of help, but that transfers arise in part from more deeply-penetrating trajectories, and may be more sensitive to potential differences.

The first such study, by Nadasen and collaborators,[11] is a follow-up to the 210-MeV elastic data described above, and was designed to ask whether inelastic data for ^{6}Li on ^{12}C, ^{28}Si and ^{58}Ni can, over the same angular range, distinguish between elastically-equivalent potentials. Their answer, in this case, is no. Put more quantitatively, for $^6Li+^{28}Si$, their elastically-determined potentials are elastically equivalent out to $\theta=31°$ (meaning that good data beyond 31° could distinguish between them), whereas these same potentials yield DWBA inelastic cross sections (to the 1.75 MeV state of ^{28}Si) which begin to deviate only at 37°. Similarly, for the ^{12}C target the elastic deviation angle is 30° and the inelastic one (to the 4.44 MeV state of ^{12}C) is 32°, so in both cases the inelastic scattering is slightly *less* sensitive to potential differences than the elastic.

A second example is provided by work of Bohlen *et al.*,[12] who also measured inelastic scattering to the 4.44 MeV state in ^{12}C, in this case in $^{12}C+^{12}C$ scattering at $E_{lab}=240$ MeV. Their elastic scattering showed a shallow farside minimum at 40°, followed by a broad 50° maximum, which was sufficient to eliminate ambiguities and determine a unique optical potential by itself. A coupled-channel calculation of collective inelastic scattering then produced essentially this same minimum-maximum structure for the 4.44 MeV angular distribution, thus indicating nearly the same interference between an inner ($b\approx3$ fm) and an outer ($b\approx5.5$ fm) trajectory as in the elastic case. The predicted 50° maximum, however, was unambiguously missing in the data. A variety of tests finally lead these authors to the conclusion that the usual dV/dr collective form factor was simply wrong in this case, and that an acceptable fit to both the elastic and inelastic data could be achieved only by the use of an inelastic form factor much more narrowly peaked around the surface, at $b\approx5$ fm, in order to suppress the inner, $b\approx3$ fm, trajectory. Thus in this case the inelastic data did not aid in determining the entrance-channel optical potential, but only in specifying more accurately the radial location of the inelastic reaction.

It is perhaps worthwhile noting in passing that the entrance-channel optical potential which resulted from

this coupled-channel search on elastic and inelastic data was nearly identical to the potential which gave the best one-channel optical fit to the elastic data alone. The only difference was a 14% reduction in the depth of the imaginary potential—and this in spite of the fact that the coupling of the 4.4 MeV state to the ground state is strong. This seems typical behavior for these "transparent" systems: the success of a one-channel optical fit is clear evidence that a coupled-channel fit will not change the entrance channel potential significantly, and so will suffer from the same discrete-ambiguity problem as the one-channel fit.

Finally, what about transfer reactions? Bohlen *et al.*[12] also measured both $^{12}C(^{12}C,^{13}C)^{11}C$ to two states of ^{13}C, and $^{12}C(^{13}C,^{12}C)^{13}C$ to two states of ^{12}C. DWBA calculations using their (unique) elastically-determined potentials, provided acceptable fits, with clear suggestions of the same 40° minimum and 50° broad maximum as in the elastic angular distributions, thus indicating distinctive interference between the same $b \approx 3$ fm and $b \approx 5.5$ fm trajectories as in the elastic case.

Satchler[5] has recently also done DWBA calculations of the $^{12}C(^{12}C,^{13}C)^{11}C$ ground-state transfer, at several bombarding energies, and finds the greatest sensitivity to potential parameters at the highest energy considered, 85 MeV/A. In particular, two moderately transparent potentials, with $(V_0, W_0) = (129,48)$ MeV and (174,28) MeV, both provide acceptable fits to the available 85 MeV/A elastic data out to $\theta \approx 20°$, but produce DWBA transfer angular distributions which differ markedly for $\theta > 5°$. The angular distribution of the second, more attractive, potential deviates from that of the first for $\theta > 5°$ because of the appearance in it of a broad (Airy?) maximum centered at 8°. Transfer data at this energy are not yet available for comparison.

The conclusion thus seems to be that one-nucleon transfers among these "transparent" nuclei receive significant contributions from both peripheral and inner trajectories, and that, although they are the same trajectories as in the elastic scattering, their interference may be sufficiently different in the elastic and transfer cases to permit transfer data to distinguish between elastically-equivalent potentials.

As for the usefulness of coupled channel searches, these studies suggest that inelastic scattering will be of little help in eliminating elastic potential ambiguities, and a coupled-channel search on elastic, inelastic, and transfer data simultaneously would require a coupled *reaction* channel search code; as far as we are aware, such a code is not currently available.

IX. CONCLUSIONS

The occurrence of a farside, or nuclear, rainbow in an angular distribution is direct evidence for low-l transparency, for its brightside Airy minima arise from an interference between low-l and peripheral-l contributions to the scattering amplitude. If only these brightside minima, but not the darkside falloff, are accessible in a given angular distribution measurement (either because the darkside of the rainbow is beyond 180° at that energy, or because the measurements are restricted to forward angles), more than one optical potential may be found to fit the data. The "true" farside cross section will exhibit one or more Airy minima in this case, and the various equivalent or ambiguous potentials will differ according to which ones of their Airy minima they choose to put at the positions of the empirical minima. These different choices provide what we refer to as the "rainbow shift" interpretation of the discrete potential ambiguity.

In most of the discrete ambiguity cases we are aware of, including all those examined in this study, the role of either the Airy minima or maxima is not at all evident without a nearside/farside decomposition of their scattering amplitudes, because they are buried invisibly under Fraunhofer oscillations. In spite of being invisible, Airy maxima provide the *éminences grises* behind discrete ambiguities, and our essential message is simply that both Airy maxima and minima are important even when invisible. Furthermore, their systematics result directly from the low-l $\delta \rightarrow (\delta + n\pi)$ shift of Drisko *et al.*, and they thus serve to emphasize the unusual transparency of certain light nucleus-nucleus combinations.

On the other hand, if the values of $Z_1 Z_2$ and the energy are propitious, it is possible for a farside rainbow to occur "in full view", with its rainbow angle Θ_R forward of 180° but beyond the Fraunhofer crossover. In this fortunate case the first brightside Airy maximum may be clearly visible, free of Fraunhofer oscillations, and it was Goldberg who first called attention to the importance of its unmistakable (provided very small cross sections can be measured) darkside falloff, using his $\alpha + ^{58}Ni$ data as an example.[2] The angular position of this falloff (i.e., the value of the rainbow angle Θ_R) is of course uniquely determined by the optical potential, and locating it is still the only known means of resolving discrete ambiguities.

The importance of the Airy minima also suggests the possible usefulness of an "Airy-order" terminology for classifying the members of a set of equivalent potentials. The A_1 or order-1 potential would be the weakest potential which fits a given angular distribution, i.e., the one with the smallest rainbow angle, which puts the *first* brightside Airy maximum A_1 at the position of the largest-angle "hump" seen in the data (or in its farside cross section), whereas the order-2 potential (stronger) would put its *second* Airy maximum A_2 there, and so have a larger (negative) rainbow angle. It is essentially just this ambiguity which was recently discussed by the Berlin group of Stiliaris *et al.*,[13] who concluded that their $^{16}O + ^{16}O$ data demanded an order-2 potential.

Finally, it is perhaps worth noting that the use of truly peripheral reactions like collective inelastic scattering generally cannot help to resolve such ambiguities, for by definition these reaction amplitudes have even weaker small-l contributions than do the elastic amplitudes. Consequently they should exhibit no farside rainbow effects at all, and to the best of our knowledge, none have ever been seen. Transfer reaction form factors, on the other hand, may penetrate deeply enough to aid in resolving discrete ambiguities, if measured at angles well beyond the grazing peak; this possibility has recently been discussed by Satchler.[5]

ACKNOWLEDGMENTS

We wish to thank Dr. A. Nadasen for sending us a numerical listing of his data, and Dr. S. H. Fricke for providing helpful semiclassical calculations of scattering amplitudes. This work was supported in part by the National Science Foundation and by CONACYT, Mexico, Grant PCCBNA-022683.

[1]R. M. Drisko, G. R. Satchler, and R. H. Bassel, Phys. Lett. **5**, 347 (1963).

[2]D. A. Goldberg and S. M. Smith, Phys. Rev. Lett. **29**, 500 (1972).

[3]A. Nadasen, M. McMaster, G. Gunderson, A. Judd, and S. Villanueva, Phys. Rev. C **37**, 132 (1988); A. Nadasen *et al., ibid.* **39**, 536 (1989).

[4]M. E. Brandan and G. R. Satchler, Nucl. Phys. **A487**, 477 (1988); M. E. Brandan, Phys. Rev. Lett. **60**, 784 (1988).

[5]G. R. Satchler, Nucl. Phys. **A505**, 103 (1989).

[6]M. E. Brandan, S. H. Fricke, and K. W. McVoy, Phys. Rev. C **38**, 673 (1988); S. H. Fricke, M. E. Brandan, and K. W. McVoy, *ibid.* **38**, 682 (1988).

[7]R. C. Fuller, Phys. Rev. C **12**, 1561 (1975); M. S. Hussein and K. W. McVoy, Prog. Part. Nucl. Phys. **12**, 103 (1984).

[8]D. A. Goldberg, S. M. Smith, H. G. Pugh, P. G. Roos, and N. S. Wall, Phys. Rev. C **7**, 1938 (1973).

[9]M. E. Brandan, M. Rodriguez-Villafuerte, and A. Ayala, Phys. Rev. C **41**, 1520 (1990).

[10]N. Rowley, H. Doubre, and C. Marty, Phys. Lett. **69B**, 147 (1977).

[11]A. Nadasen, M. McMaster, M. Fingal, J. Tavormina, J. S. Winfield, R. M. Ronningen, P. Schwandt, F. D. Bechetti, J. W. Jänecke, and R. E. Warner, Phys. Rev. C **40**, 1237 (1989).

[12]H. G. Bohlen, X. S. Chen, J. G. Cramer, P. Fröbrich, B. Gebauer, H. Lettau, A. Miczaika, W. von Oertzen, R. Ulrich, and T. Wilpert, Z. Phys. A **322**, 241 (1985).

[13]E. Stiliaris, H. G. Bohlen, P. Fröbrich, B. Gebauer, D. Kolbert, W. von Oertzen, M. Wilpert, and Th. Wilpert, Phys. Lett. B **223**, 291 (1988).